Very High spatial Resolution IR thermography diagnostic positioning system upgrade in WEST Tokamak

L. Dubus, M. Houry, C. Pocheau, X. Courtois, Mh. Aumeunier, S. Vives

Very High spatial Resolution IR thermography diagnostic positioning system upgrade in WEST Tokamak

L. Dubus, M. Houry, C. Pocheau, X. Courtois, MH. Aumeunier, S. Vives
CEA-IRFM, F-13108 Saint-Paul-Lez-Durance, France

Abstract. The Very High spatial Resolution (VHR) infrared thermography diagnostic developed by CEA-IRFM is installed in the WEST tokamak to measure surface temperature of the actively cooled W-monoblocks (MB) of the Plasma Facing Units (PFUs), which are similar to the International Thermonuclear Experimental Reactor (ITER) ones. It is a major diagnostic to investigate the behaviour of PFU during experimentation thanks to its very high spatial resolution (0.1 mm / pixel), movable field of view (FoV) and the wide-range temperature measurement. In particular, it can study the evolution of monoblocks mounted in the tokamak, the influence of the shaping of these components submitted to high heat load and the behaviour of the leading edges regarding the assembling tolerances between adjacent monoblocks. Finally, such diagnostic directly contributes to the specification assessment of the ITER divertor units. This diagnostic was operational during the 2019 WEST experimentation and its enhanced design for the 2020 WEST experimentation campaign. In order to monitor 30x12mm monoblocks temperature, the VHR IR diagnostic is able to move its narrow FoV (64x51mm) to specific targets on the observable divertor area (360×420mm). Position and focus steering are achieved through motor-controlled mirrors and lenses operated by a dedicated Labview application on a remote unit. Mirror positioning occurs between pulses under normal WEST operation conditions, and can withstand thermal radiation and disruptions during pulses. Repeatability, hysteresis, mechanical components reliability are critical parameters to provide accurate positioning (<1mm) of the FoV. The tuning and calibration of these actuators in accordance with WEST environment is crucial to guarantee the best position of the FoV and optical performances. This paper gives the FoV positioning implementation details and performance of the VHR in WEST.

1 Introduction & context

The CEA-IRFM WEST tokamak is equipped with a full tungsten divertor of thousands of monoblocks that offers a great testing platform for ITER's future divertor [1], [2]. This major piece of equipment is designed to receive ITER-relevant heat flux from 10MW/m² to 20MW/m² at peak. Thus, small misalignments can induce misplaced heat loads and finally damage monoblocks [3]. Therefore, study of leading edges and monoblock gaps is crucial to ensure integrity of different geometries.

In 2018, CEA-IRFM developed the Very High spatial Resolution (VHR) infrared thermography diagnostic which is a one-of-a-kind system [4], [5], [6] that provides surface temperature data with 0.1mm/pixel resolution [7] and movable field of view (FoV). It led to successful results, [8], [9], [10], [11] and studies in plasma-wall interaction [12], [13], [14], [15]. Such accomplishments require a highly performant equipment with a reliant positioning system.

2 Description of the diagnostic

2.1 Tokamak environment

The WEST divertor with the ITER-like Plasma Facing Units (PFUs) is a conical surface at the bottom of the vacuum vessel. The observation on the divertor is made from an upper port. The line of sight between the first mirror and the divertor is about 2m, with an incidence close to 90° (Figure 1). This incidence angle is dependent of the FoV position as the divertor has an inclination of 21° relative to the ground and a toroidal shape. Such dimensions doesn't deform the resulting IR image.

The head of the endoscope which contains the first mirrors is positioned 30cm backward in the port to prevent the heat load deposition from particles and to reduce the radiative flux.

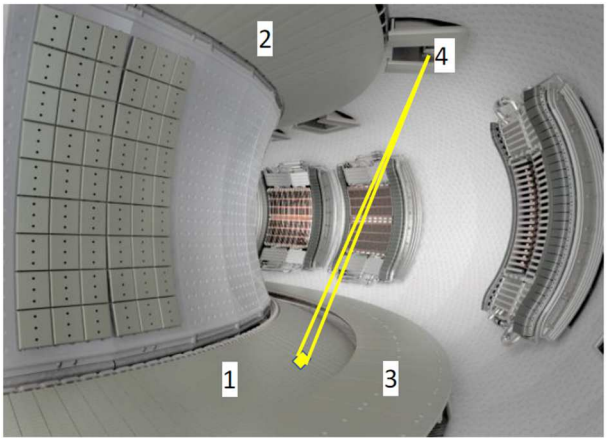

Figure 1 CAD view of the WEST Vessel. (1) lower divertor (2)upper divertor, (3) Baffle, (4) upper port with VHR diagnostic.

It provides a movable FoV of 64 x 51 mm on an observable area of 360 × 420 mm covering a grid of 17 PFUs by 30 monoblocks (see Figure 2). The average size of a monoblock is 30 x 12 mm. It goes from PFU #7 of the sector Q3B to PFU #22 and from monoblock 10 to 30. Such distance and resolution specification (0.1mm/pixel) requires a high performance FoV positioning system.

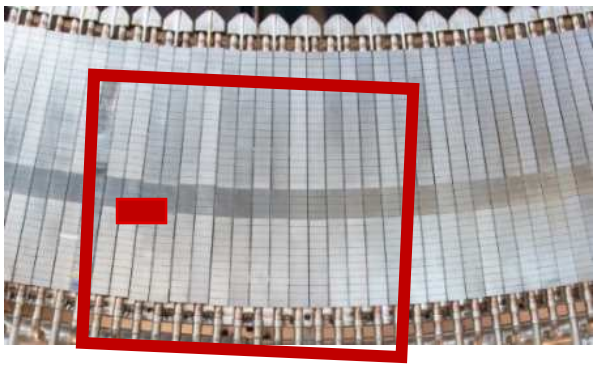

Figure 2 The observable area on the WEST divertor (large red rectangle) and the VHR moving FoV (small red plain rectangle)

2.2 Endoscope overview

High accuracy positioning demands a vibration resilient structure, which is provided by a light and stiff space-inspired mechanical design. The VHR endoscope features vibrational modes higher than 50 Hz, which makes it almost insensitive to the main mechanical vibrations in the tokamak environment.

In order to reach such high spatial resolution, the diagnostic optical design is composed of 6 mirrors and 4 lenses (see Figure 3): 1 spherical mirror (#3), a cylindrical mirror (#4), 4 lenses and 4 flat mirrors (#1, #2, #5, #6) [7]. The endoscope has a CEA-IRFM home-made IR camera [17] at the top, located ex-vessel, with a resolution of 640x512 pixels for a final 64x51mm FoV.

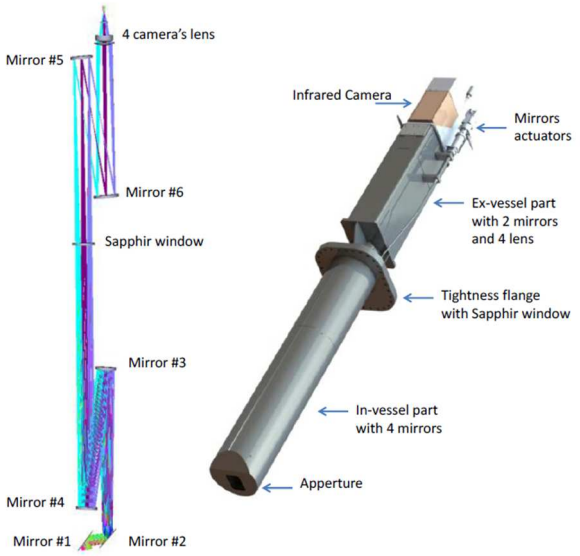

Figure 3 CAD view of the optical path and global VHR IR diagnostic

2.3 FoV positioning opto-mechanical initial design

The FoV positioning mirrors M1 and M2 (located in the in-vessel part of the endoscope) rotate on their axis to provide respectively toroidal and poloidal moving directions (see Figure 4). They are actuated by stepper motors located at the upper end of the endoscope (outside of the vacuum vessel, next to the IR camera) through stainless steel cable (see Figure 3).

M1 and M2 have an angular range limitation of [-1°; +1°], an angular precision of 0.005° and a cable amplitude of 2.5mm. Hard limit switches located at the stepper motor level provide safety run stops to ensure the right positioning of mirrors and avoid the reduction of image brightness toward the periphery compared to the image center (vignetting). In addition, mechanical bumpers safeguard the rotation movement to prevent from completely going off specification. Piezoelectric motors were firstly considered but couldn't be implemented due to the high magnetic field (>1T) present in the tokamak hall.

(a)

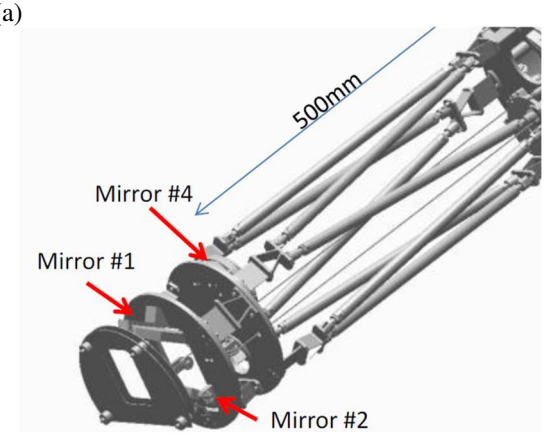

(b)

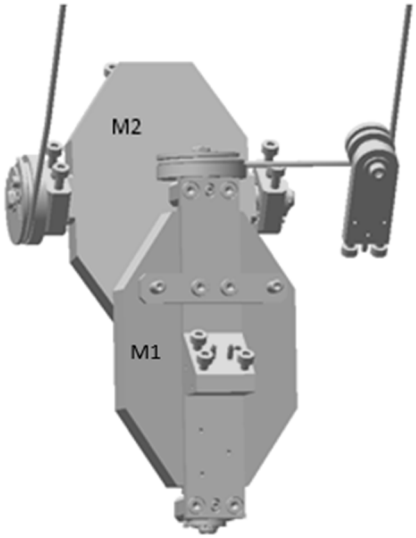

Figure 4 (a) Mechanical design of the lower part of the endoscope. (b) CAD view of mirror rotating axis actuated by stainless steel cable via pulleys

The pulleys allow guidance of the stainless steel cable to the mirror rotation axis which embeds a return spring giving the counter-reaction needed for moving on the other direction (see Figure 5).

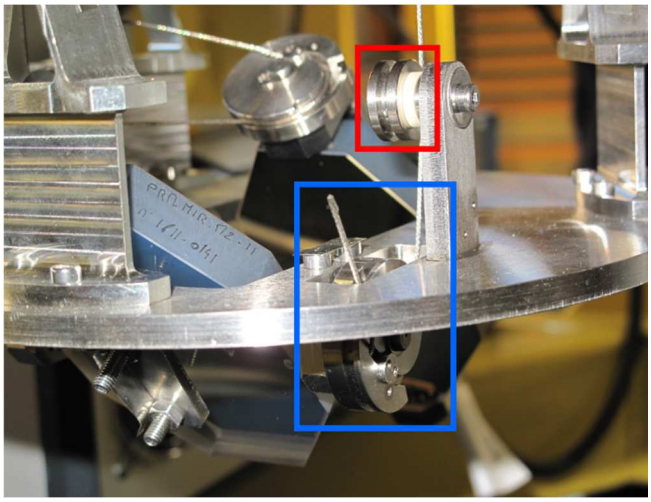

Figure 5 Close up image of the mechanical system to position facing mirrors. The pulley (red rectangle) guiding the stainless steel cable to the mirror rotating axis (blue rectangle) embedding the return springs.

2.4 Performance of the initial design

FoV positioning performance characterization has been carried out through a dedicated test bench in laboratory. The endoscope is mounted on a specialized caddie with a divertor mockup rule at the system focus distance. It is a metallic plate with graduated marks on the edges and predrilled holes with IR sources, representing monoblocks.

It is crucial to determine the linearity of the whole system response before proceeding to the calibration per se. The FoV is moved on the divertor replica and the travelled distance is read from the graduated ruler on the IR image retrieved. This operation is performed for the whole frame in both directions ('+' and '-') for both motors (M1 and M2).

As Figure 6 shows, there is a 33% hysteresis on the toroidal direction between the travelled distance of the FoV and the needed motor steps. It has been measured on both motors and at different locations on the mockup. This nonlinear behavior is due to numerous factors: the small amplitude of the cable actuating the rotation of mirrors (2.5mm), the cable elasticity under such amplitude and the pulley friction against the cable.

Residual between the two paths is calculated to characterize the impact of the hysteresis in Equation 1:

$$residual_i = abs\left(\frac{d_{+_i} - d_{-_i}}{\overline{m_i}}\right) \qquad (1)$$

Where:

- d_+: travelled distance from reference in the '+' direction
- d_- : travelled distance from reference in the "-" direction
- $\bar{m}$: motor step average of both direction

Equation 1 Hysteresis residual metric to measure mechanical performance

It can reach up to 8.2 µm/step of deviation with this design which led to a significant uncertainty on the FoV positioning. Giving an error in the order of magnitude of up to 4 MBs in the toroidal direction and 3 MBs in the poloidal direction.

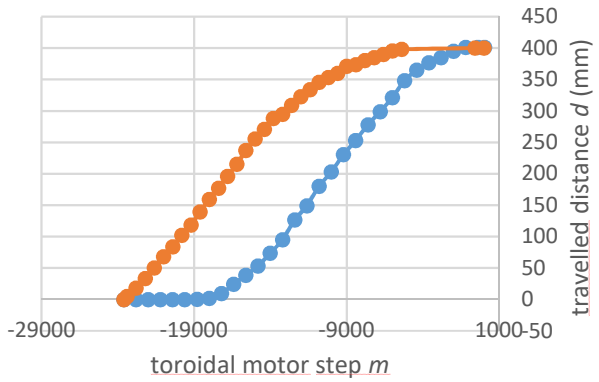

Figure 6 Travelled path towards PFU20 (orange) and back, towards PFU7 (blue) of the FoV on toroidal direction (M1).

This hysteresis has been compensated in the driving software during WEST campaigns C3 and C4, to target proper monoblock. The FoV was always returning to the closest edge to initialize the beginning of the wanted move. This method had doubled the amount of points needed for calibration as it requires to be processed for both directions for each motors.

Overall, it was impractical and needed an expert to move the FoV with confidence. Therefore, an upgraded design has been developed to simplify calibration, driving and processing of the whole system.

3 Upgraded design

3.1 Mechanical enhancement

In order to get rid of the hysteresis and improve the FoV positioning accuracy, the simplest way is to increase the amplitude of the stainless steel cable to minimize its elasticity impact on the actuation. The mirrors actuation system has been entirely redesigned and a new larger pulley has been added to make a higher lever as shown in Figure 7. This increases the cable amplitude from 2.5mm to 15mm. The initial cable has also been replaced by a multi-strand one featuring a higher stiffness. It has been mechanically creeped before mounting to reduce its long term strain.

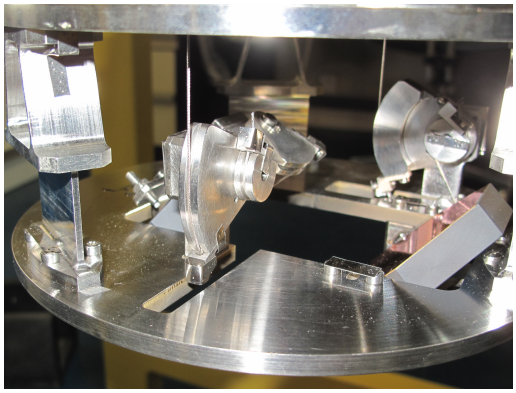

Figure 7 Upgraded mechanical system with increased cable amplitude through augmented pulley leverage.

3.2 Performance of the upgraded design

The experimental performance of the enhanced design gives substantial better results, as shown in Figure 8, where the system has an insignificant hysteresis, with a maximum residual of 2.0 µm/step. The system is then 4 times more performant than the initial design and offers a maximum absolute deviation on the travelled path of 176µm. The gain ratio is not equal to the amplitude gain of 15/2.5 certainly because of residual backlash of the whole system (cable elasticity, small mechanical slack, hard limit switch tolerance).

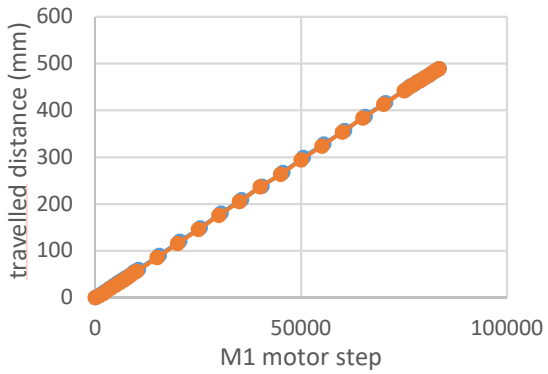

Figure 8 Travelled path for the upgraded VHR positioning system

This improvement in the system response implies directly better accuracy on the targeted monoblock. Indeed, it has been validated through an endurance test that runs the FoV to a specific target multiple times on the mockup. First, it starts from the origin of the motor domain, in the left hand corner of the observable area, at coordinates (0,0). Then, it goes to a specific monoblock. Once the FoV has finished its run, an IR movie is recorded. The IR sources in the predrilled hole serves as markers for data analysis. This operation is repeated 10 times for a set of PFU/monoblock in the observable area: PFU{7,13,21} and MB{10,20,30}. In data analysis, each circle center is then detected by computer vision and compared with all of the others runs (see Figure 9). It gives the error in both directions (poloidal and toroidal).

The maximum displacement in the poloidal direction is 80 pixels * 0.1mm/pixel = 8mm. Following the same reasoning, the maximum toroidal positioning error is 3mm. Such errors are under the dimension of one 30x12mm monoblock, so it is ensured that the expected target will always be on frame.

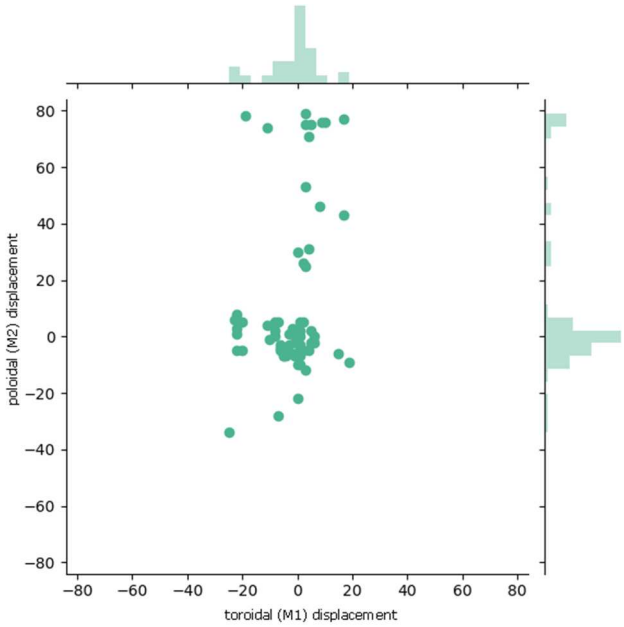

Figure 9 Distribution of monoblock center in the IR image after endurance tests of 100 runs. The displacement is in pixels. Bar graphs on the axis edges correspond to the displacement statistical distribution.

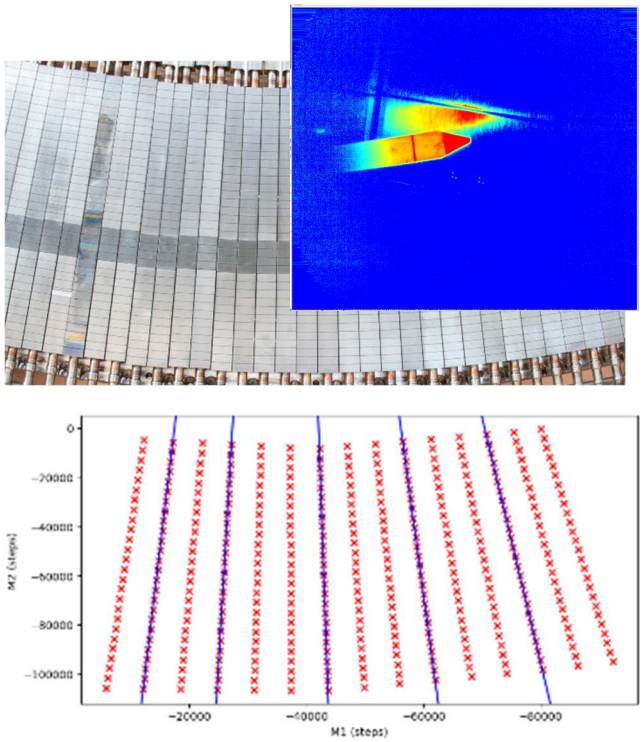

Figure 10 Calibration and extrapolation process. Position measurements of MB center is carried out in-situ on a set of point to form a grid and reference lines (in blue), which are then extrapolated to the whole observable area.

4 Moving towards monoblocks

4.1 Spatial Calibration

The main issue for a correct FoV positioning in WEST is that there is nothing more like a monoblock than a monoblock. The FoV actuation system is calibrated with a process done in-situ during tokamak maintenance. A set of monoblock is selected to shape a grid that is extrapolated afterwards to the whole observable area. An IR source is pointed on the center of a monoblock, then the operator moves the FoV until it sees the IR source in the middle of the screen. 9 reference points are needed to ensure a correct spatial calibration but the more points are added, the more robust the calibration becomes.

As described in Figure 10, poloidal and toroidal motor coordinates are mapped against each other. Reference lines parameters are estimated from reference points read along a PFU. The toroidal shape of the divertor allows to estimate the center of the machine thanks to the extrapolation of those reference lines. Once estimated, it is used as the new origin in a polar domain to interpolate the radius corresponding to the monoblocks (12mm in that poloidal direction) in each PFU containing the reference lines. After that, the missing PFUs are linearly interpolated to fill the grid inside the experimental points. And finally, an extrapolation is performed to predict out of bounds monoblocks.

4.2 WEST exploitation

The VHR IR diagnostic is operational from the control room. Indeed, a Labview dedicated application uses the above mentioned calibrated grid for an automatized FoV positioning. Nevertheless, the application also allow a manual adjustment of the FoV position if required.

5 Conclusion

In the context of tokamak fusion machine and plasma-wall interaction studies, with its various unique environmental constraints (>1T magnetic field, mechanical stress generated by disruptions, vibrations in the machine), the Very High Resolution at 0.1mm/pix designed with its movable FoV offers great capabilities in terms of specialized tool in this field. Indeed, with the mechanical system upgrade (cable amplitude increased to 15mm), the positioning accuracy is more resolved (8mm poloidal, 3mm toroidal) than the size of one monoblock (30x12mm). The positioning system of the diagnostic is easier to maintain, more reliable and available.

This new system is operational on WEST since 2020 to provide necessary measurements for the study of leading edges and gaps during high heat load deposit on ITER-like monoblocks. With relevant measurements and its extrapolation algorithm, the whole observable

area (400x500mm) in the divertor sector Q3B of WEST can be monitored.

Some improvements are being studied, such as increasing motor speed for faster operation while keeping same positioning performance, adding a feedback sensor to give motor current position and increase reliability on movement and consolidate monoblock position through image recognition algorithm on edges and shapes.

Acknowledgments

This work has been carried out within the framework of EUROfusion Consortium and has received funding from Euratom research and training programme. The views and opinions expressed herein do not necessarily reflect those of the European Commission.

References

[1] J. Bucalossi, M. Missirlian, P. Moreau, F. Samaille, E. Tsitrone, D. Houtte, T. Batal, C. Bourdelle, M. Chantant, Y. Corre, X. Courtois, L. Delpech, L. Doceul, D. Douai, H. Dougnac, F. Faïsse, C. Fenzi, F. Ferlay, M. Firdaouss et J.-M. Travere, «The WEST project: Testing ITER divertor high heat flux component technology in a steady state tokamak environment,» *Fusion Engineering and Design,* vol. 89, pp. 907-912, October 2014.

[2] S. Carpentier-Chouchana, T. Hirai, F. Escourbiac, A. Durocher, A. Fedosov, L. Ferrand, M. Firdaouss, M. Kocan, A. S. Kukushkin, T. Jokinen, V. Komarov, M. Lehnen, M. Merola, R. Mitteau, R. A. Pitts, P. C. Stangeby et M. Sugihara, «Status of the ITER full-tungsten divertor shaping and heat load distribution analysis,» *Physica Scripta,* vol. T159, p. 014002, April 2014.

[3] Y. Corre, J.-L. Gardarein, R. Dejarnac, J. Gaspar, J. P. Gunn, M.-H. Aumeunier, X. Courtois, M. Missirlian et F. Rigollet, «Methodology for heat flux investigation on leading edges using infrared thermography,» *Nuclear Fusion,* vol. 57, p. 016009, October 2016.

[4] R. E. Nygren, D. L. Rudakov, C. Murphy, J. D. Watkins, E. A. Unterberg, J. L. Barton et P. C. Stangeby, «Thermal management of tungsten leading edges in DIII-D,» *Fusion Engineering and Design,* vol. 124, p. 271–275, November 2017.

[5] B. Sieglin, M. Faitsch, A. Herrmann, B. Brucker, T. Eich, L. Kammerloher et S. Martinov, «Real time capable infrared thermography for ASDEX Upgrade,» *Review of Scientific Instruments,* vol. 86, p. 113502, November 2015.

[6] P. Vondracek, E. Gauthier, O. Ficker, M. Hron, M. Imrisek et R. Panek, «Fast infrared thermography on the COMPASS tokamak,» *Fusion Engineering and Design,* vol. 123, p. 764–767, November 2017.

[7] M. Houry, C. Pocheau, M.-H. Aumeunier, C. Balorin, K. Blanckaert, Y. Corre, X. Courtois, F. Ferlay, J. Gaspar, S. Gazzotti, A. Grosjean, T. Loarer, H. Roche, A. Saille et S. Vives, «The very high spatial resolution infrared thermography on ITER-like tungsten monoblocks in WEST Tokamak,» *Fusion Engineering and Design,* vol. 146, pp. 1104-1107, 2019.

[8] Y. Corre, A. Grosjean, J. P. Gunn, K. Krieger, S. Ratynskaia, O. Skalli-Fettachi, C. Bourdelle, S. Brezinsek, V. Bruno, N. Chanet, J. Coenen, X. Courtois, R. Dejarnac, E. Delmas, L. Delpech, C. Desgranges, M. Diez, L. Dubus, A. Durif, A. Ekedahl, N. Fedorczak, M. Firdaouss, J.-L. Gardarein, J. Gaspar, J. Gerardin, C. Guillemaut, M. Houry, T. Loarer, P. Maget, P. Mandelbaum, R. Mitteau, M. Missirlian, P. Moreau, R. Nouailletas, E. Nardon, C. Pocheau, A. Podolnik, P. Reilhac, X. Regal-Mezin, C. Reux, M. Richou, F. Rigollet, J.-L. Schwob, E. Thorén, P. Tolias et E. Tsitrone, «Sustained W-melting experiments on actively cooled ITER-like plasma facing unit in WEST,» *Physica Scripta,* vol. 96, p. 124057, November 2021.

[9] A. Grosjean, Y. Corre, J. Gaspar, J. P. Gunn, S. Carpentier, X. Courtois, R. Dejarnac, E. Delmas, G. D. Temmerman, M. Diez, L. Dubus, L. Dupont, F. Escourbiac, M. Firdaouss, J. Gerardin, M. Houry, R. Pitts, C. Pocheau et E. Tsitrone, «Very high-resolution infrared imagery of misaligned tungsten monoblock edge heating in the WEST tokamak,» *Nuclear Materials and Energy,* vol. 27, p. 100910, June 2021.

[10] A. Grosjean, M. H. Aumeunier, Y. Corre, M. Firdaouss, J. Gaspar, J. Gerardin, J. P. Gunn, X. Courtois, R. Dejarnac, M. Diez, L. Dubus, M. Houry, C. Pocheau et E. Tsitrone, «Interpretation of temperature distribution observed on W-ITER-like PFUs in WEST monitored with a very-high-resolution IR system,» *Fusion Engineering and Design,* vol. 168, p. 112387, July 2021.

[11] A. Grosjean, Y. Corre, R. Dejarnac, J. Gaspar, J. P. Gunn, S. Carpentier-Chouchana, X. Courtois, E. Delmas, G. D. Temmerman, M. Diez, L. Dubus, A. Durocher, F. Escourbiac, M. Firdaouss, J. Gerardin, M. Houry, R. A. Pitts, C. Pocheau et E. Tsitrone, «First analysis of the misaligned leading edges of ITER-like plasma facing units using a very high resolution infrared camera in WEST,» *Nuclear Fusion,* vol. 60, p. 106020, September 2020.

[12] M. Diez, Y. Corre, E. Delmas, N. Fedorczak, M. Firdaouss, A. Grosjean, J. P. Gunn, T. Loarer, M. Missirlian, M. Richou, E. Tsitrone et the WEST Team, «In situ observation of tungsten plasma-facing components after the first phase of operation of the WEST tokamak,» *Nuclear Fusion,* vol. 61, p. 106011, September 2021.

[13] J. P. Gunn, J. Bucalossi, Y. Corre, M. Diez, E. Delmas, N. Fedorczak, A. Grosjean, M. Firdaouss, J. Gaspar, T. Loarer, M. Missirlian, P. Moreau, E. Nardon, C. Reux, M. Richou et E. Tsitrone, «Thermal loads in gaps between ITER divertor monoblocks: First lessons learnt from WEST,» *Nuclear Materials and Energy,* vol. 27, p. 100920, June 2021.

[14] M. Diez, J. P. Gunn, M. Firdaouss, A. Grosjean, Y. Corre, E. Delmas, L. Gargiulo et E. Tsitrone, «First evidence of optical hot spots on ITER-like plasma facing units in the WEST tokamak,» *Nuclear Fusion,* vol. 60, p. 054001, April 2020.

[15] M. Richou, Y. Corre, T. Loewenhoff, M. Diez, C. Martin, A. Aretz, J. W. Coenen, M. Firdaouss, G. Giacometti, A. Grosjean, G. Pintsuk, H. Roche, M. Spähn, G. D. Temmerman, E. Tsitrone, M. Wirtz et the WEST Team, «First plasma exposure of a pre-damaged ITER-like plasma-facing unit in the WEST tokamak: procedure for the PFU preparation and lessons learned,» *Nuclear Fusion,* vol. 62, p. 056010, March 2022.

[16] A. Grosjean, «Impact of geometry and shaping of the plasma facing components on hot spot generation in tokamak devices,» 2020.

[17] X. Courtois, M. H. Aumeunier, C. Balorin, J. B. Migozzi, M. Houry, K. Blanckaert, Y. Moudden, C. Pocheau, A. Saille, E. Hugot, M. Marcos et S. Vives, «Full coverage infrared thermography diagnostic for WEST machine protection,» *Fusion Engineering and Design,* vol. 146, p. 2015–2020, September 2019.